Published in final edited form as:
Chem Res Toxicol. 2009 July ; 22(7): 1285–1297. doi:10.1021/tx9000896.

Effect of Cross-Link Structure on DNA Interstrand Cross-Link Repair Synthesis

Michael B. Smeaton[‡], **Erica M. Hlavin**[‡], **Anne M. Noronha**[#], **Sebastian P. Murphy**[#], **Christopher J. Wilds**[#], and **Paul S. Miller**[*]
Department of Biochemistry and Molecular Biology, Johns Hopkins Bloomberg School of Public Health, Johns Hopkins University, 615 North Wolfe Street, Baltimore, MD 21205, USA

Abstract

DNA interstrand cross-links (ICLs) are products of chemotherapeutic agents and cellular metabolic processes that block both replication and transcription. If left unrepaired, ICLs are extremely toxic to cells, and ICL repair mechanisms contribute to the survival of certain chemotherapeutic resistance tumors. A critical step in ICL repair involves unhooking the cross-link. In the absence of a homologous donor sequence, the resulting gap can be filled in by a repair synthesis step involving bypass of the cross-link remnant. Here we examine the effect of cross-link structure on the ability of unhooked DNA substrates to undergo repair synthesis in mammalian whole cell extracts. Using ^{32}P incorporation assays, we found that repair synthesis occurs efficiently past the site of damage when a DNA substrate containing a single N^{4}C-ethyl-N^{4}C cross-link is incubated in HeLa or CHO cell extracts. This lesion, which can base pair with deoxyguanosine, is readily bypassed by both *E. coli* DNA polymerase I and T7 DNA polymerase in a primer extension assay. In contrast, bypass was not observed in the primer extension assay or in mammalian cell extracts when DNA substrates containing a N3T-ethyl-N3T or N1I-ethyl-N3T cross-link, whose linkers obstruct the hydrogen bond face of the bases, were used. A modified phosphorothioate sequencing method was used to analyze the ICL repair patches created in the mammalian cell extracts. In the case of the N^{4}C-ethyl-N^{4}C substrate, the repair patch spanned the site of the cross-link and the lesion was bypassed in an error-free manner. However, although the N3T-ethyl-N3T and N1I-ethyl-N3T substrates were unhooked in the extracts, bypass was not detected. These and our previous results suggest that although the chemical structure of an ICL may not affect initial cross-link unhooking, it can play a significant role in subsequent processing of the cross-link. Understanding how the physical and chemical differences of interstrand cross-links affect repair may provide a better understanding of the cytotoxic and mutagenic potential of specific interstrand cross-links.

INTRODUCTION

Interstrand cross-links (ICLs) are one of the most disruptive types of lesions formed in DNA because they block essential cellular processes such as transcription and replication (1). The formation of such lesions is the basis for the toxicity of many drugs commonly used to treat cancer. ICLs are also formed by agents derived from endogenous and environmental sources (2,3). In cancer cells, repair of ICLs is an undesired mechanism by which tumors can acquire resistance to anticancer drugs (4), whereas in normal cells, repair pathways might be necessary to protect the cell from the deleterious consequences of these lesions. There is wide variation in the chemical structures of ICLs that are formed from chemotherapeutic, endogenous or

*Correspondence should be addressed to Paul S. Miller, E-mail: pmiller@jhsph.edu, Phone: (410)-955-3489, Fax: (410)-955-2926.
‡These authors contributed equally to this work
#Department of Chemistry and Biochemistry, Concordia University, Montreal, Quebec, Canada

environmental sources. It is not clear, however, how the physical and chemical properties of a given ICL affect the ability of the cell to repair such a complex form of DNA damage.

ICL repair in *Escherichia coli and Saccharomyces cerevisiae* involves an initial unhooking step that releases the ICL from one of the DNA strands, leaving a cross-link remnant attached to the other stand. This step is mediated by the nucleotide excision repair (NER) pathway in both organisms (5,6). Further processing of the unhooked DNA involves a repair synthesis step in which the gap created by unhooking is filled in. In the presence of homologous DNA, homologous recombination (HR) provides an undamaged template for faithful repair synthesis (1,6,7). However, homologous recombination-independent pathways have been observed in bacteria, yeast and mammals, which utilizes translesion synthesis (TLS) to bypass the cross-link remnant (8–13). In *E. coli*, DNA Polymerase I is a required factor for removal of ICLs, where it appears to play a role in the lesion bypass step (14,15) and in yeast, polymerase ξ is involved in bypass during G1 phase (12).

Repair of ICLs in mammalian cells is quite complex, and many different repair pathways and proteins have been implicated including NER (9,10,16,17), HR (8,18,19), TLS (20–22), mismatch repair (MMR) (23–25), Fanconi anemia associated proteins (26), Mus81 (27) Werner helicase (28,29) and many more (1). Similar to yeast, the pathways used to repair ICLs may depend on the phase of the cell cycle, and there is significant evidence that homologous recombination-independent pathways exist that utilize lesion bypass to process ICLs in mammalian cells (9,10,13,23,24).

It has been shown that in mammalian cell extracts, the NER pathway makes dual incisions on the 5’ side of an ICL creating a gap that undergoes a futile repair synthesis process that does not result in removal of the cross-link (16,30,31). We have recently reported on a pathway in mammalian cell-free extracts that unhooks ICLs in a DNA substrate that is undergoing neither transcription nor replication (30). The efficiency of unhooking depended on the level of helix distortion induced by the ICL, but not on the chemical structure of the cross-link. Surprisingly, functional NER was not required for unhooking.

In this report we further examine processing of cross-linked DNA in HeLa and hamster whole cell extracts and show that the extracts, subsequent to unhooking, carry out repair synthesis on this substrate. We demonstrate that, in contrast to the unhooking reaction, the ability to carry out repair synthesis is dependent upon the chemical structure of the ICL.

EXPERIMENTAL PROCEDURES

Materials

Protected deoxyribonucleoside 3′-O-phosphoramidites, 5′-biotin phosphoramidite and oligonucleotide synthesis reagents were obtained from Glen Research, Inc. Protected deoxyribonucleoside-3′-O-methylphosphonamidites were a product of JBL, Inc. Polynucleotide kinase, T4 DNA ligase, *E. coli* DNA polymerase I (Klenow fragment), and T7 DNA polymerase were obtained from New England Biolabs, Inc. Shrimp alkaline phosphatase (SAP) was from Roche Diagnostics. Reactions employing these enzymes were carried out in buffers supplied by the manufacturer. High performance liquid chromatography (HPLC) was performed on a Varian instrument using a 0.4 × 25 cm Dionex strong anion exchange (SAX) column. MALDI-TOF mass spectrometry was performed on an Applied Biosystems Voyager mass spectrometer at the AB Mass Spectrometry/Proteomics Facility of the Johns Hopkins School of Medicine, with support from the National Center for Research Resources Shared Instrumentation, Grant 1S10-RR14702.

Substrate Preparation

The structures of the N^4C-ethyl-N^4C (C-C, -CG- or -GC- orientation), N3T-ethyl-N3T (T-T), N1I-ethyl-N3T (I-T), or a 4′-aminomethyl-4,5′,8-trimethyl-psoralen (AMT) interstrand cross-links (ICLs) and their placement in linear double-strand DNA substrates are shown schematically in Figure 1A. The synthesis and purification of the cross-linked duplexes containing the various ICLs have been described (32–35). Oligonucleotides used to prepare the full-length cross-linked substrates are shown in Table S1 and were synthesized as previously described (36). The duplex generically referred to as **X** in Table S1 was ligated into the center of the full-length duplex and contained either no damage, a 1,3-GTG intrastrand platinum lesion or one of the interstrand cross-linked duplexes. The full length duplex substrates for all assays are ~150 base-pairs, but each duplex **X** (see Table S1) varies slightly in length. For the sake of clarity, we will simply refer to them from here on as a 150mer.

The substrates for the α-^{32}P repair synthesis assays are shown schematically in Figure 1B and were prepared as follows. The 5'-end of the top strand of the **A** duplex (see Table S1) was labeled using γ-^{32}P ATP (100 Ci/mmol) and T4 PNK and this labeled strand was annealed with its complementary strand to form the duplex. Labeled duplex **A** was then ligated with the other duplexes shown in Table S1 to create the 150mer substrate (36, 37). The ligation reactions were run on a 6% denaturing PAGE gel, and the full-length ligation product was identified, excised from the gel and extracted overnight at 37°C with a solution consisting of 20% acetonitrile in 0.1 M ammonium acetate, pH 6.2. The DNA was then precipitated and dissolved in 1X shrimp alkaline phosphatase (SAP) buffer, annealed by slow cooling from 90°C, and the concentration determined by scintillation counting. The substrates were then treated with SAP in order to remove the terminal 5' ^{32}P label. The substrates used in the α-^{32}P repair synthesis assay as well as the phosphorothioate sequencing analyses contained terminal 3' biotins that, when conjugated to streptavidin, block the ends of the duplex. This has been shown to increase nucleotide excision repair signals in mammalian cell extracts (36). Streptavidin conjugated duplexes were prepared by incubating 50 fmol of duplex with streptavidin (1 mg) overnight at 4°C.

^{32}P-Labeled substrates for the phosphorothioate sequencing assays (structures shown schematically in Figure 1C) were prepared by ligating duplex **A**, whose top strand was 5'-end labeled at 6000 Ci/mmol, with the appropriate duplexes shown in Table S1 as described above. After gel purification, the full-length substrate was precipitated and dissolved in a 1X TE buffer containing 100 mM KCl. Each duplex was annealed by slow cooling from 90°C, and its concentration determined by scintillation counting. The labeled duplexes were then conjugated with streptavidin as described above.

For the primer extension assays, an 18 nucleotide (nt) long primer and 36 nt templates containing either no damage, a C-C cross-link remnant, or a T-T cross-link remnant (see Figure 2A and B) were synthesized on an ABI 3400 DNA/RNA synthesizer using standard phosphoramidite chemistry and were purified by HPLC. The cross-link remnants were incorporated using either the N^4C-ethyl-N^4C or N3T-ethyl-N3T phosphoramidites that were synthesized and purified as previously described (33, 34). The primer and template compositions were confirmed by MALDI-TOF mass spectrometry: primer *m/z* expected 5529.67, *m/z* found 5529.14; C-C template *m/z* expected 11225, *m/z* found 11226.84; T-T template *m/z* expected 11255, *m/z* found 11254.53.

The ^{32}P-labeled -GC- cross-linked substrate used to characterize the unhooked product (see Figure 1D) was prepared by ligating duplex **A'**, which contains 6 contiguous methylphosphonate linkages at the 5' end and a 3' biotin, and duplex **F'**, which contains 6 contiguous methylphosphonate linkages at the 3' end and a 5' biotin, with the other duplexes **B, C, X(-GC-), D**, and **E** (see Table S1). The top strand of duplex **D** was labeled with ^{32}P prior

to ligation. ICL remnant-containing size markers (shown schematically in Figure 1E) used to characterize the unhooked product were prepared by ligating duplexes **A', B, C, X+1** or **X+2, D, E**, and **F'**. The 5'-end of the top strand of the **D** duplex contained a ^{32}P label. Duplex **X+1** contains the N^{4}C-ethyl-N^{4}C cross-link remnant in its upper strand, whereas duplex **X+2** contains the N^{4}C-ethyl-N^{4}C cross-link remnant with an additional guanine attached to the 5' side to the cross-linked cytosine. A non-damaged marker was also prepared by ligating duplexes **A', B, C-X, D, E,** and **F'**. Because the duplexes resulting from these ligations are not cross-linked, they migrate as single-stranded 150mers on a denaturing polyacrylamide gel and therefore are represented as labeled single strands in Figure 1E. The top strands of duplexes **X+1** and **X+2** were synthesized as follows. Oligonucleotide **X+1A** was prepared on the synthesizer (1 μmol scale, 25 mg of controlled pore glass support) with a O^4-triazole-U at the position of C. The 5'-end of the support-bound oligonucleotide was acetylated and the support-bound oligonucleotide was incubated with a 200 μL of a 0.3 M solution of 5'-O-dimethoxytrityl-3'-O-*t*-butyldimethylsilyl-N^4(2-aminoethyl)deoxycytidine (38) in anhydrous pyridine for 96 h at 45°C. The reagents were removed by washing the support with 2 mL of pyridine followed by 3, 10 mL portions of acetonitrile and the support was dried under vacuum. A portion of the support was deprotected by treatment with 400 μL of a solution containing 95% ethanol/concentrated ammonium hydroxide (1:3 v/v) for 3.5 h at 55°C. The oligonucleotide, which still retained a *t*-butyldimethylsilyl (TBS) group, was purified by C-18 reversed phase HPLC. The TBS group was then removed by treating the oligonucleotide with triethylamine trihydrofluoride overnight at room temperature. The oligonucleotide was then desalted on a C-18 reversed phase cartridge. The composition of **X+1A** was confirmed by MALDI-TOF mass spectrometry: *m/z* expected 3545, *m/z* found 3544.4. The remaining support was detritylated and coupled with protected deoxyguanosine-3'-O-phosphoramidite using standard coupling conditions. The oligonucleotide, **X+2A**, was deprotected as described above and purified by SAX HPLC. The composition of the **X+2A** was confirmed by MALDI-TOF mass spectrometry: *m/z* expected 3874.7, *m/z* found 3874.4.

Primer extension assays

Primer extension assays using the Klenow fragment of *E. coli* Pol I (Kf) and T7 DNA polymerase were performed using templates containing either no damage, a N^{4}C-ethyl-N^{4}C cross-link remnant, or a N3T-ethyl-N3T cross-link remnant. The primer oligonucleotide was 5'-end labeled using T4 PNK and γ-^{32}P ATP at a specific activity of 10 Ci/mmol and unincorporated label was removed using a G-25 size-exclusion column. A 2.5 μM solution of both the 18 nt 5' ^{32}P-labeled primer and a 36 nt template were annealed at 25°C for 30 minutes in 10 μL of 1X NEB buffer #2 (Kf) or T7 DNA polymerase buffer and then incubated with 100 μM dNTPs and 2.5 units of Kf or 5 units of T7 DNA polymerase at 25°C. Aliquots (1μL) were removed at 0, 15, and 90 minutes and the reactions were quenched by adding to 9 μL of denaturing loading buffer (80% formamide, 0.05% xylene cyanol and 0.05% bromophenol blue) followed by immersion in a boiling water bath for 1 minute. The reaction products were analyzed on a 20% denaturing PAGE gel. The gel was exposed to a phosphorimage screen which was scanned using a Fuji Film FLA-7000.

Cell culture and preparation of whole cell extracts

HeLa, wild-type CHO AA8 cells (AA8), NER-deficient UV41 (XPF), and UV135 (XPG) cells were grown as previously described (30). Extracts were prepared from ~10^9 cells using the method of Manley (39) with previously described modifications (37). The protein concentrations of the extracts were determined to be 15–20 mg/mL using the Bio-Rad protein assay system.

Characterization of the unhooked product

Unhooking reactions were carried out as described previously (30) for 4 hours on the -GC- cross-linked substrate whose structure is shown schematically in Figure 1D. The unhooked, 150mer single-stranded product was excised and extracted from the gel as described above. The mobility of the unhooked product was compared to a number of standards that either contained no damage, a single cytosine attached to the cross-link (**+1**), or a CG attached to the cross-link (**+2**). All of the standards were the same length as the top strand of the -GC- substrate and contained the same terminal methylphosphonate linkages (shown schematically in Figure 1E). The unhooked product was dephosphorylated with SAP in order to remove any phosphate on the cross-link remnant. This step was necessary because all of the cross-linked standards contained a cross-link remnant with no 5' phosphate. The standards were treated the same as the -GC- unhooked product in order to control for differences in handling. The unhooked product and standards were then precipitated and analyzed on a pre-run (1.5 hours) 6% sequencing PAGE gel (45 cm × 20 cm × 0.4 mm) at 1800 V until the xylene cyanol tracking dye was 19 cm from the bottom of the gel. The gel was fixed in a solution containing 5% methanol, 5% acetic acid, and 90% water for 5 min, dried on a gel dryer and exposed to a phosphorimage screen overnight.

α-^{32}P Repair synthesis assays

Repair synthesis was monitored by measuring incorporation of an α-^{32}P labeled dNTP as previously described (40). The reactions were performed in silanized 1.5 mL Eppendorf tubes in 25 μL of a buffer containing 25 mM HEPES, pH 7.9, 4.4 mM magnesium chloride, 0.1 mM EDTA, 1 mM dithiothreitol, 70 mM potassium chloride, 4 mM ATP, 200 μg/mL bovine serum albumin, 2.5–5% glycerol, 160 μM of dTTP, dCTP, dGTP, 8 μM of dATP and 5 μL (75–100 μg) of HeLa, AA8 or XPF whole-cell extract. Reactions were set up and held on ice for 10 minutes; initiated by the addition of 20 fmol of substrate and 3 μCi of α-^{32}P-dATP; then incubated at 30°C for 90 minutes. The reactions were stopped by adding 10 μg of proteinase K containing 0.3% SDS, followed by incubation for 15 min at 37°C. The reaction mixtures were then extracted with phenol/chloroform/isoamyl alcohol (25:24:1 v/v) followed by chloroform/isoamyl alcohol (24:1) using Phase Lock gel tubes (Eppendorf). Samples were ethanol precipitated and analyzed on a 18 × 20 cm 6% denaturing polyacrylamide gel run at 60°C to examine for full length single stranded 150mer products and on an 8% denaturing sequencing gel to monitor truncated products (~70–75 nt). Where indicated, aphidicolin dissolved in DMSO was added to a final concentration of 100 μM and control samples were treated with an equivalent amount of DMSO.

Phosphorothioate sequencing

The phosphorothioate sequencing method was carried out as previously described (40–43) with some modifications described below. Briefly, 5' ^{32}P end-labeled non-damaged or cross-linked substrates (shown schematically in Figure 1C) were incubated under reaction conditions similar to those described above for the α-^{32}P repair synthesis assays. Five separate reactions were set up for each experiment, one control in the presence of all four normal dNTPs (160 μM) and four reactions each with three dNTPs (160μM) and one dNTPαS (160μM). Equal amounts of protein were used for each reaction. The reactions were incubated at 30°C for 90 minutes and processed as described above. Samples were ethanol precipitated and separated on a 18 × 20 cm 6% denaturing PAGE run at 60°C to identify the single-stranded 150mer product, which was excised and extracted from the gel slice as described above. The DNA was subsequently ethanol precipitated, dissolved in 9 μL of water and treated with 1 μL of a 5 mM solution of iodine (dissolved in 100% ethanol) for 1 minute at 25°C. This step hydrolyzes the phosphorothioate linkages created when the α-thiophosphate dNTPs were incorporated during repair synthesis. The short cleavage time with iodine allows partial hydrolysis to occur such

that each position of incorporated α-thiophosphate dNTP can be read. The recovered oligonucleotides underwent an additional ethanol precipitation and were analyzed on a 12% denaturing sequencing gel to determine the sequence of the ICL repair patch. Quantification of the repair patches was done using Multi Gauge 3.0 software. For each nucleotide within the repair patch, the intensity of the band that resulted from iodine cleavage was plotted as a percentage of the total incorporation divided by how many times that nucleotide was incorporated. Graphs were plotted using Sigma Plot 9.0.

RESULTS

Interstrand cross-linked DNA duplexes

Figure 1A shows the chemical structures of the cross-links, their abbreviations, and a schematic showing their orientation in the DNA duplex. Included are a N^4C-ethyl-N^4C cross-link arranged in a mismatched C-C or a staggered -CG- or -GC- orientation, a N3T-ethyl-N3T (T-T), and a N1I-ethyl-N3T (I-T) cross-link, both in mismatched orientations, and a psoralen cross-link. Although the exocyclic amino groups of the cytosines of the N^4C-ethyl-N^4C cross-link are joined by an ethyl linker, these amino groups can still participate in hydrogen bond formation with a complementary guanine. On the other hand, the ethyl linkers attached to the N3 or N1 atoms of the T-T and I-T cross-links obstruct the hydrogen bonding face of the base and therefore would be expected to interfere with pairing to a complementary base.

Figures 1B-D shows schematics of the cross-linked 150bp linear DNA duplexes and Figure 1E shows schematics of the cross-link remnant modified 150nt single-stranded DNA markers used in our studies. The 3'-ends of the duplexes shown in Figure 1B and 1C were derivatized with a biotin/streptavidin conjugate. This modification prevents the Ku70/80 heterodimer from binding to the ends of the linear duplex and blocks degradation by 3'-exonucleases. We have previously shown that the magnitude of NER excision repair signal in mammalian cell extracts is enhanced when Ku70/80 binding is prevented by this modification (36). In order to monitor ICL unhooking and characterize the unhooked product, the 3' and 5'-ends of the upper strand of the duplex shown in Figure 1D were modified with 6 methylphosphonate linkages. The methylphosphonate linkages are resistant to nucleases and thus protect the unhooked strand from exonuclease degradation. The methylphosphonate linkages in combination with the 3' and 5' biotin/streptavidin conjugate also prevent end-binding by Ku70/80. The cross-linked DNA duplexes and the cross-link remnant single-stranded DNA markers were synthesized by methods reported previously (30, 33, 34, 38, 44).

Effect of cross-link remnants on DNA polymerase-mediated primer extension

Primer extension assays were used to determine if and how the structure of a cross-link remnant affects the ability of DNA polymerase to bypass this type of lesion when embedded in a template strand. Single-stranded templates were synthesized that contained a single N^4C-ethyl-N^4C or N3T-ethyl-N3T remnant as shown schematically in Figure 2A. The remnant, which consists of a single C or T residue attached to a C or T residue in the template via an ethyl linker, has the same structure as the cross-link remnant observed after cross-link unhooking in mammalian whole cell extracts (see below). Each modified template was annealed to a 5'-^{32}P-labeled primer whose 3'-end is six bases removed from the cross-link remnant. The sequences of the template and the primer are shown in Figure 2B where X in the template strand denotes either no damage (a cytosine), the N^4C-ethyl-N^4C or the N3T-ethyl-N3T remnant.

As shown in Figure 2C, *E. coli* Pol I Klenow fragment exo+ (Kf) was able to extend 43% of the primer to the end of the non-damaged (ND) template in 90 minutes under the conditions described in Materials and Methods. When the N^4C-ethyl-N^4C template was used, the

polymerase was also able to extend 54% of the primer to the end of the template after 90 minutes, indicating Kf was able to bypass this cross-link remnant efficiently. Furthermore, we observe similar bypass efficiency by Klenow exo- and the kinetics of full-length primer extension on the N^4C-ethyl-N^4C template versus the ND template are similar (see Figure S1 and Figure S2). There does, however, appear to be a buildup of product that results due to pausing at position 28, four bases past the cross-link site (see Figure 2C and Figure S2). However, there is also a slight pause at the same position in the non-damaged template of identical sequence, indicating that the sequence at that location may cause the polymerase to pause at position 28.

In contrast to the N^4C-ethyl-N^4C remnant, the N3T-ethyl-N3T remnant served as a potent block to Kf-mediated primer extension as indicated by the presence of a truncated product that migrates as a 24mer (Figure 2C). This truncated product indicates that DNA polymerization occurred up to the N3T-ethyl-N3T remnant site and stalled at the base directly before the lesion. The substrates used for these primer extension studies all have the same sequence. Therefore it is the ICL structure, and not the surrounding DNA sequence, that ultimately results in polymerase blockage. This block was essentially complete, as the amount of the only larger oligonucleotide generated, which migrated as a 35mer, was very minor. This 35mer is one nucleotide shorter than the full-length 36mer template and most likely results from a small amount of oligonucleotide that did not incorporate the N3T-ethyl-N3T cross-link amidite during synthesis and therefore acts as a 35mer non-damaged template. The Kf exo- also produced a minor product that migrated as a 25mer, one nucleotide longer than the stall site observed by Kf exo+ (Figure S2). This is likely due to non-templated 3’ additions known to occur with Kf exo- after the primer disassociates from the template.

Similar results were observed when T7 DNA polymerase was used in the primer extension assay. As shown in Figure 2D, T7 DNA polymerase was able to efficiently bypass the N^4C-ethyl-N^4C cross-link remnant and extend the primer to the end of the template (16%) in a manner similar to the non-damaged substrate (18%). However, the N3T-ethyl-N3T remnant completely blocked extension by T7 DNA polymerase. As was the case with Kf, polymerization occurred up to the base directly preceding the cross-link but no base was placed across from the cross-link remnant.

Characterization of unhooked product structure generated in mammalian extracts

We recently reported that human and hamster whole cell extracts are capable of unhooking a variety ICLs, including those shown in Figure 1, embedded in a linear 150bp DNA duplex (30). Cross-link unhooking, which did not depend upon proteins of the NER pathway, produced a single-stranded 150mer that contained the remnant of the cross-link. We have now further characterized the structure of the unhooked product because the number of bases attached to the remnant has been shown to influence DNA polymerase bypass activity (45,46).

A 150bp linear DNA duplex containing a single -GC- oriented N^4C-ethyl-N^4C ICL (shown schematically in Figure 1D) was incubated in human (HeLa) or hamster (AA8) whole cell extract for 4 hours and the unhooked product was purified by gel electrophoresis. The unhooked product was then treated with alkaline phosphatase to remove any 5’ phosphate groups because the monoadducted standards are synthesized without any 5’ phosphates on the remnant. The electrophoretic mobility of the unhooked oligonucleotide was then compared to the mobilities of standards with identical length and end-modifications that contained either no damage (**ND**), a cross-link remnant with a single cytosine (**+1**), or a cross-linked remnant with 5’-GC (**+2**). Figure 1E shows schematic representations of these standards, and their sequences are provided in Table S1. As shown in Figure 3 the unhooked product, **U**, generated by either the HeLa (Figure 3A) or AA8 (Figure 3B) extract has a mobility that is clearly greater than that of the **+2** standard and similar if not identical to that of the **+1** standard. This result is consistent

with a structure in which the cross-link remnant contains a single cytosine attached to the non-incised strand through the ethyl linker of the cross-link as shown schematically in Figure 3C. Although we think it unlikely, this assay does not rule out the possibility that the sugar and/or base of this residue has undergone further modification.

Figure S3 demonstrates that even after 1.5 hrs of incubation in mammalian whole cell extracts, the product generated by unhooking contains a single nucleotide. We have shown previously that in our extracts there is minimal random exonucleolytic degradation of the NER dual excision products in this time frame (see Figure S4 in reference (30)). These results suggest that a specific exonuclease processing step may remove any nucleotides remaining on either side of the cross-link after the initial unhooking.

Repair synthesis of interstrand cross-linked duplexes in mammalian cell extracts

Cross-link unhooking creates a potential substrate for repair synthesis. The gap that results from unhooking the cross-link can be filled in by a DNA polymerase using the cross-link remnant-containing strand as a template, and the nick that remains after polymerization can be sealed by DNA ligase to produce a full length 150mer. In order to determine if repair synthesis takes place after unhooking in mammalian cell extracts, non-labeled 150bp linear duplexes were prepared that contained 3'-terminal biotin/streptavidin conjugates as shown schematically in Figure 1B. These duplexes, whose sequences are shown in Table S1, contained either no damage, a 1,3 (GTG) platinum intrastrand lesion (Pt), a N^4C-ethyl-N^4C ICL in either a mismatch C-C, -CG- or -GC- orientation, a N3T-ethyl-N3T ICL, a N1I-ethyl-N3T ICL or an aminomethyltrimethyl psoralen (AMT) ICL. The duplexes were incubated in HeLa or CHO whole cell extracts supplemented with α-^{32}P-NTPs and the products were analyzed by denaturing gel electrophoresis. As shown in Figure 4A, when the non-damaged duplex was incubated with either HeLa or CHO cell extract, very little incorporation of radioactivity was observed. In contrast, incubation of the duplex containing the Pt lesion, resulted in significant incorporation of ^{32}P label to generate a labeled 150mer oligonucleotide. The labeled 150mer results from NER-mediated excision of the platinum lesion in the form of a platinated oligonucleotide 27–29 nucleotides in length followed by repair synthesis of the resulting gap as previously described (40).

When the -CG- or the -GC- cross-linked duplexes were incubated in the whole cell extracts, a single-stranded 150mer oligonucleotide was observed as shown in Figure 4A. The appearance of this 150mer ^{32}P-labeled product is consistent with fill-in of the gap created after cross-link unhooking and subsequent ligation. The greater incorporation of ^{32}P -label into 150mer product derived from the -GC-cross-linked duplex is consistent with our previous observation that the distorted -GC- cross-link is unhooked to an approximately 10-fold greater extent than the non-distorted -CG- cross-link (30). Furthermore, as shown in Figure S4, formation of the labeled 150mer was observed when the cross-linked duplex was incubated in an NER-deficient XPF extract, demonstrating that repair synthesis, like cross-linking unhooking, occurred in a NER-independent manner. The XPF extract is completely devoid of excision activity on the 1,3 platinum lesion, although it can be complemented with an NER-deficient XPG extract (see ref (30)). Together these observations indicate that the fill-in step to generate the 150mer occurs in response to the unhooking reaction we observed previously (30).

In addition to the 150mer product, labeled material was observed near the top of the gel. There are at least three explanations that should be considered: i) nick-translation/ligation labels genomic DNA that is present in the extract, ii) nick-translation/ligation labels the substrate, or iii) dual 5' NER incision/ligation labels the substrate. When dNTPs and α-^{32}P-dATP are incubated with extract alone (no substrate), the high molecular weight material still appears, while the 150mer single-strand does not (data not shown). Therefore the bulk of the material near the top of the gel would appear to result primarily from non-specific labeling of genomic

DNA. However, labeled cross-linked material also runs in this region of the gel. Hence, processes ii) or iii) may occur to some degree, but their products would be largely obscured by the labeled genomic DNA. In order to avoid interference by this material, sequencing of the ICL repair patch in Figure 5 and Figure 6 was done exclusively on gel purified 150mer single-stranded product.

Although both of the -GC- and C-C cross-linked duplexes produced the 150mer repair synthesis product when incubated in AA8 cell extract, the 150mer was not observed when the T-T, I-T or psoralen cross-linked duplexes were incubated under the same conditions, as shown in Figure 4B. Considering that all of these substrates undergo cross-link unhooking in the AA8 extract (30), these results suggest that, unlike the N^4C-ethyl-N^4C cross-link, the structures of the T-T, I-T and psoralen cross-links interfere with repair synthesis in mammalian whole cell extracts.

The ethyl linkers of T-T and I-T cross-links project from the hydrogen bond face of the base, and could block the progress of polymerases attempting to fill in the gap created by cross-link unhooking. Similar to the primer extension reactions described above (see Figure 2), such blockage would be expected to result in the formation of truncated, ^{32}P-labeled products. To test this possibility, the C-C and T-T cross-linked duplexes were incubated in an XPF-deficient extract in order to eliminate the NER-dependent futile repair synthesis, and the products of the reaction were analyzed on a sequencing gel as shown in Figure 4C. Consistent with the results presented in Figures 4A and 4B, the C-C cross-linked duplex produced a single 150mer product (data not shown). No shorter products were observed that would indicate stalling at the site of the cross-link remnant (Figure 4C). In contrast, repair synthesis of the T-T cross-linked duplex generated two products, a 70mer and a 74mer (Figure 4C), whose sizes were established as described in Figure S5. As shown in Figure 4D, the lengths of these products are consistent with polymerization up to the site of the cross-link remnant on either the upper (70 nt band) or lower (74 nt band) strand. These results indicate that the DNA polymerases present and active in mammalian whole cell extracts stall at the site of the T-T cross-link. This behavior is similar to that of a psoralen cross-link (Figure 4B), where it was observed that repair synthesis in AA8 cell extracts does not occur past the cross-link remnant (31). Although the psoralen cross-link remnant does not block the hydrogen bond-face of T per se, the adduct may be sufficiently bulky to prevent polymerization past this lesion.

Direct sequencing of ICL repair patches in mammalian cell extracts

A modified version of a phosphorothioate sequencing method previously employed to analyze NER repair patches (40,42,43) was used to characterize the location of the repair synthesis patch generated on the N^4C-ethyl-N^4C cross-linked duplexes. This method exploits the ability of iodine to cleave the thiophosphate linkages created when α-thiophosphate modified nucleotides are incorporated into the repair patch during repair synthesis. The sequence of the entire repair patch can be determined by carrying out four separate reactions, each containing a different α-thio-dNTP. This method is especially useful for analyzing repair patches arising from interstrand cross-links because both the location and fidelity of repair synthesis can be monitored simultaneously.

Repair synthesis was carried out on the 150mer -CG- and the -GC- cross-linked duplexes shown in Figure 1C. Each duplex carried a single 5'-^{32}P-label on one of the 5' terminal ends. Four separate reactions were carried out for each duplex in which the duplex was incubated in AA8 whole cell extract for 90 min in the presence of one of the four α-thio-dNTPs and the other three d-NTPs. The 150mer product from each reaction was gel purified after electrophoresis, treated with iodine to cleave at the positions of thiophosphate incorporation and analyzed by sequencing gel. As shown in Figure 5, a specific patch of nucleotides was incorporated into each duplex. This patch is distinct from that of the non-specific background synthesis that is

observed over the entire length of the duplex when a non-damaged duplex is subjected to the same reaction conditions (see Figure S6).

Repair synthesis resulted in incorporation of a complementary guanine (indicated by the circled band in the gel shown in Figure 5B), opposite the N^4C-ethyl-N^4C remnant. Furthermore, at least at these detection limits, it appeared that no other base was placed opposite this lesion. These results suggest that the template was faithfully copied to generate a -CG- or -GC- sequence at the site of the cross-link, depending on which duplex was examined.

Characterization of NER-independent repair patch

The repair patch shown in Figure 5A appears to extend from approximately the 28th nucleotide 5' to the ICL to about the 4th nucleotide 3' of the ICL as indicated by the sequence on the right hand side of the gel. The size of the patch suggests that it results from repair synthesis at gaps produced by both the NER-dependent 5'-dual incisions and the NER-independent cross-link unhooking reaction. At first this seems unreasonable because sequencing was carried out on a full-length 150mer, and as noted above, futile repair synthesis, which occurs after the NER-dependent 5'-dual incisions (16, 31) would produce a 5'-end labeled oligonucleotide less than 75 nucleotides in length. However, Sancar and colleagues observed that a portion (~10%) of the population of molecules undergoing futile repair synthesis undergo ligation to regenerate the original cross-linked duplex (31). If this duplex, which would now contain phosphorothioate linkages, was subsequently unhooked, it would then run as a 150mer on the gel and consequently be sequenced. Although the number of molecules that experience NER-mediated dual 5' incisions, repair synthesis, ligation, and unhooking would be expected to be low, we reason that the sensitivity of the phosphorothioate sequencing assay is sufficiently high to enable the dual 5' incision repair patch to be observed.

To test this possibility, we carried out the phosphorothioate sequencing assay in an XPF-deficient extract. This extract, which lacks NER activity, is completely incapable of excising a 1,3-Pt intrastrand lesion. However excision activity is restored when the extract is complemented with an XPG extract (30). The XPF and XPG extract preparations display an equal level of unhooking activity on a given ICL substrate (30). When the -CG- or -GC- cross-linked duplex was incubated in a reaction mixture containing the complemented XPF and XPG extracts supplemented with α-thio-dGTP or α-thio-dCTP, repair patches similar to those seen in the wild-type extracts were observed as shown in Figure 6A. However, when the cross-linked duplexes were incubated in the XPF-deficient extract alone, the size of the repair patch decreased. This can be seen more easily in Figures 6B–E where the percentage of radioactivity in each band on the gel is plotted as a function of its position relative to the cross-link, which is located at position 0. In the XPF extract, there is a significant decrease of the signal that is normally generated in the wild-type extracts starting at position −28 (28 bases 5' to the ICL). This decrease is consistent with loss of the repair synthesis patch generated from the NER-dependent dual 5' incisions. As a consequence, a smaller synthesis patch is created that starts at about the 3rd nucleotide 5' of the ICL lesion and diminishes after the 4th or 5th nucleotide 3' of the ICL. There is some background synthesis observed in the XPF extract 5' to the ICL where the NER dual incisions occur in wild-type extracts. This may be due to polymerase back tracking from the NER independent 5' incision location before polymerization. In the XPF mutant, the fill-in is less intense in this 5' region relative to that seen with the XPF+XPG extract (see graphs in Figure 6), however, qualitatively, the pattern is the same because the sequences of the substrates are identical. The locations of the 5' and 3' ends of this NER-independent repair patch agree closely with those of the previously observed incisions that give rise to unhooking, a further indication that the repair synthesis patch arises in response to the NER-independent unhooking (30).

DISCUSSION

Bifunctional agents that create ICLs in DNA form the basis for many chemotherapeutic treatments (1). Such agents include psoralen compounds, mitomycin C, nitrogen mustards, BCNU, platinum compounds and others. ICLs can also be formed by endogenous and environmental sources. These include those that arise from the byproducts of lipid peroxidation such as malondialdehyde (47,48), acrolein, crotonaldehyde, and 4-hydroxy-2E-nonenal (HNE) (49,50). Nitric oxide (51) and abasic sites (52) have also been demonstrated to create DNA ICLs. The ICLs formed by these different agents vary widely in chemical structure and likely have significantly different effects on the structure of the DNA helix in which they are embedded. Repair of ICLs requires many steps to remove the damage from both strands of the DNA duplex, and there are many different repair pathways and proteins implicated in mammalian ICL repair. Evidence from studies in *E. coli* and *S. cerevisiae* indicates that repair of these lesions in the absence of a homologous donor sequence involves an initial unhooking step followed by repair synthesis as shown schematically in Figure 7A (8,14,53). The latter step requires polymerase bypass of the cross-link remnant that resides on the intact strand followed by ligation to seal the remaining nick. The cross-link remnant could then be removed in a second round of repair by the NER pathway. There is significant evidence in mammals that homologous recombination-independent and lesion bypass-dependent pathways exist to repair ICLs (9,10,13,24,53).

Although the initial cross-link unhooking step in bacteria and yeast is mediated by the NER pathway, the situation may be different in mammalian cells. As shown schematically in Figure 7B, in mammalian cell extracts, the NER pathway makes dual incisions 5’ to the site of the ICL, but these incisions do not lead to unhooking of the ICL (16, 30, 31). We have found that interstrand cross-linked duplexes that are not undergoing transcription or replication are unhooked in mammalian cell extracts by an activity that does not use NER proteins (30). Unhooking is stimulated by increasing levels of helix distortion induced by the ICL, but does not appear to depend on the chemical structure of the cross-link itself.

The specific mechanisms of ICL repair may depend largely on the context in which an ICL is encountered. For instance, a number of lines of evidence suggest that during replication, the NER pathway as a whole does not appear to play a major role in initiation of repair of ICLs (19,54,55). Most rodent NER mutant cell lines display only slightly enhanced sensitivity relative to wild-type, while XPF and ERCC1 mutants were significantly sensitive and appear not to be able to unhook the cross-links as measured by a modified comet assay (19). This has implicated a special role for the XPF-ERCC1 nuclease in ICL repair outside of its traditional role as 5’ endonuclease for the entire NER pathway. When a site-specific ICL is placed into a plasmid with a replication origin, repair was observed to be independent of the NER pathway (54). Studies with recombinant XPF-ERCC1 have shown it is able to unhook cross-linked substrates that are placed in forked, but not linear, structures *in vitro* (56,57). The formation of ICL-induced double-strand breaks during S-phase, however, is independent of XPF-ERCC1 (58). Recent work has demonstrated a role for XPF-ERCC1 in double strand break repair (59), further complicating analysis of the role of XPF-ERCC1 during unhooking in S-phase. The related structure specific nuclease Mus81-Eme1, however, is involved in the generation of double-strand breaks during ICL repair in S-phase (27). Furthermore, components of the MMR pathway appear to play a role in promoting error-free repair of ICLs (23,25). It has been shown *in vitro* that the damage recognition factors XPC-hHR23B and XPA-RPA are able to recognize psoralen ICLs (17) and, recently, that they can cooperate at the site of an ICL with MMR proteins to promote binding (25).

ICLs are potent blocks not only to replication, but transcription as well, and therefore ICL repair in a G1 context may be an important protection mechanism for cells. Indeed, yeast have

evolved a mechanism of ICL repair in G1 phase that utilizes NER and TLS (12). Repair of ICLs in G1 phase may reduce the burden of ICLs encountered by DNA polymerases during replication, and may therefore contribute to survival under conditions of high ICL stress in dividing cells. Consistent with this, ablation of the NER pathway results in increased γ-H2AX foci in cycling cells challenged with psoralen (20).

Work by Li, Legerski and co-workers (9,10), as well as by our own group (Hlavin and Miller, unpublished observations) has shown that the NER pathway is involved in repair of an ICL placed in a luciferase reporter plasmid when the plasmid is transfected into mammalian cells. In these studies, repair was shown to depend largely on the nucleotide excision repair pathway and translesion synthesis. This is illustrated in the marked decrease (~75–80%) of cross-linked plasmid reporter expression in all NER mutant cell lines tested. These studies did not suggest a special role for XPF-ERCC1 outside of normal NER. Thus it seems when measuring ICL repair during transcription, but not replication, the NER pathway can be considered dominant at some step in repair of ICLs that leads to gene reactivation. Currently, nothing is known mechanistically about unhooking of ICLs during transcription.

The substrates used in our studies on ICL repair monitor global genomic type repair of a single site-specific lesion. For instance, using the same linear duplex containing a single platinum 1,3 (GTG) intrastrand cross-link, we observe excision in mammalian extracts that is strictly dependent on the global-genomic and not transcription-coupled NER pathway (data not shown). The pathways that repair ICLs in non-transcribing, non-replicating DNA remain largely unknown, but may contribute towards repair throughout the cell cycle in all cell types.

In our studies and those of Bessho et al. in whole cell extracts using site-specific ICL substrates, the global-genomic NER pathway only makes incisions on the 5’ side of the ICL (16,30). It remains possible that *in vivo*, the NER pathway is able to unhook ICLs but the factors required for this are lost or destabilized during the process of extract preparation. It is also possible that the NER pathway can unhook cross-link structures that are created during transcription, but do not occur on the linear substrates we used in our studies. Alternatively, the NER dependent dual 5’ incisions may serve as a signal *in vivo* to recruit other repair factors as originally suggested by Sancar (16), potentially including the unhooking activity we have observed.

Using a plasmid with a site-specific psoralen ICL, Legerski and coworkers have developed a repair synthesis assay to monitor ICL repair in extracts (60). This pathway proceeds through the use of RPA and PCNA (61), two factors likely to be involved in the repair synthesis we observe here. Furthermore, they have found that MutSβ, the Werner protein (WRN) and a complex containing the E3 ubiquitin ligase Pso4/Prp19 contributes to the observed repair (62), and it is possible they too are involved in the processing we observe.

We have described a pathway that unhooks ICLs and then, depending on the cross-link structure, a TLS mechanism functions to bypass the cross-link (see Figure 7). Unhooking and bypass are independent of NER including XPF-ERCC1 (30) and the unhooking step occurs efficiently in extracts prepared from cell lines defective in the MMR and HR pathway (M. Smeaton and P. Miller, unpublished observations). Using a plasmid based recombination assay, it was shown that XPF-ERCC1 cooperates with components from the FA, HR and MMR pathways to promote a homology-dependent repair pathway of ICLs when a double strand break is formed nearby (63). Considering we do not observe the generation of any double strand breaks in our assays (30) and that we don’t provide homologous donor sequences, the lack of involvement of the MMR, HR pathways and XPF-ERCC1 is consistent with these factors promoting a homology-dependent ICL repair process described in reference (63).

The studies described in this report have used cross-linked duplexes of the types shown in Figure 1 to examine the effect of cross-link structure on repair synthesis, a step subsequent to

cross-link unhooking. As shown schematically in Figure 7C, the cytosine in the exocyclic amino group of the N^4C-ethyl-N^4C cross-link retains a hydrogen bond donor that can participate in base-pairing with an incoming guanine during DNA polymerization. Both high resolution NMR and X-ray crystallographic studies of duplexes containing a -CG- oriented N^4C-ethyl-N^4C cross-link show that the cytosines of the cross-link can base pair with their partner guanines on the complementary strands (35,64). In this sense, this cross-link is similar to the alkyl cross-links formed between the exocyclic amino groups of guanine. Such N^2G-alkyl-N^2G cross-links have been shown to arise from reaction of DNA with α, β-unsaturated aldehydes such as acrolein (49). A N^2G-trimetheylene-N^2G cross-link remnant, which mimics an acrolein ICL, can be efficiently and faithfully bypassed by human polymerase κ and *E. coli* pol IV (45,46). Consistent with these results, we have observed that the N^4C-ethyl-N^4C cross-link remnant is efficiently bypassed by *E. coli* Pol I, T7 and DNA polymerases present and active in mammalian cell extracts.

Other cross-links form chemical linkages to the adducted base at a position that blocks normal hydrogen bonding potential. For example, reaction of DNA with the chemotherapeutic agent *bis*-chloroethylnitrosourea (BCNU) gives rise to an N3C-ethyl-N1G ICL whose ethyl linker blocks the hydrogen bonding faces of both C and G. As shown schematically in Figure 7C, the ethyl linkers of the N3T-ethyl-N3T and N3T-ethyl-N1I cross-links block the hydrogen bond faces of T and I (32, 33) and thus mimic the ICL formed by BCNU. In contrast to the N^4C-ethyl-N^4C cross-links and the N^2G-trimethylene-N^2G cross-link, the N1I-ethyl-N3T and N3T-ethyl-N3T cross-links are potent blocks to DNA polymerase bypass.

The experiments described in Figure 3 show that the mammalian NER-independent unhooking reaction gives rise to a cross-link remnant with a single nucleotide attached. Interestingly, a similar cross-linked unhooked product was observed recently during replication-dependent unhooking in *Xenopus* egg extracts (65). It has been demonstrated that polymerase bypass efficiency is greatly diminished when the cross-link remnant contains additional nucleotides, particularly when they are placed on the 3'-side of the remnant (45,46). Considering the unhooking reaction we have characterized (30) is from non-replicating and non-transcribing DNA, this unhooking event may play an important role in initiating repair of endogenous ICLs formed in terminally differentiated cells. In such cell types, where a sister chromatid is not available, repair synthesis involving bypass of the cross-link remnant would be expected to be the dominant pathway. The results in Figure 3 show that after the unhooking reaction, an unhooked structure with a single nucleotide is generated; a substrate that is most amenable to bypass by DNA polymerases. Whether the unhooking reaction itself gives rise to the single nucleotide product or a subsequent exonuclease step is responsible remains to be determined. Indeed, it may be that DNA polymerase exonuclease activity is responsible for removing any attached oligonucleotide after unhooking occurs but prior to repair synthesis.

Consistent with the results from the primer extension assays, both ^{32}P-incorporation repair synthesis and the phosphorothioate sequencing assays demonstrate that after cross-link unhooking, polymerases present in mammalian cell extracts can efficiently bypass the N^4C-ethyl-N^4C cross-link remnant (Figure 4, Figure 5 and Figure 6). The phosphorothioate sequencing method proved to be an effective method to analyze both the precise location of the repair patch as well as the fidelity of ICL bypass. Repair synthesis of the -CG-, -GC- or C-C cross-linked duplexes generated a specific repair patch. What appears to be a large patch, which was observed when the duplexes were incubated with extract from wild-type cells, results from two separate processing events: the NER-dependent dual 5' incision repair patch and the NER-independent unhooking repair patch (shown schematically in Figure 7). When the duplexes were incubated with an XPF-deficient extract, a small patch was observed whose size was consistent with the NER-independent incisions that are observed on either side of the cross-link. The NER-independent incisions were observed at the 1st to the 4th nucleotides 5'

of the ICL and at the 4th through the 7th nucleotides 3' to the ICL. The repair patch observed in the XPF-deficient extract starts most strongly at the 3rd nucleotide 5' of the ICL and ends at the 4th-5th nucleotide 3' of the ICL as shown in Figure 6. These results strongly suggest that the repair patch observed in the NER-deficient extract is formed in response to the NER-independent incisions and unhooking characterized previously (30).

It should be noted here that in the work by Sancar and colleagues (31), depending on the conditions, a significant portion of the molecules that undergo 5' futile incision are re-ligated (see Figure 2 in reference (16)). If this molecule were subsequently unhooked, the resulting patch would appear to be produced by both the NER dependent and independent processing events. This seems the likely explanation because the NER dependent dual 5' incisions alone would not produce a 150mer single strand, which was gel purified before thiosequencing analysis. Dual 5' futile NER incision-synthesis-ligation prior to unhooking would also explain why the signal from the shorter unhooking patch is as strong as the Pt fill-in signal, which contains a patch of ~30 nucleotides (Figure 4). While unhooking can occur independently of the dual NER incisions (30), it remains a possibility that *in vivo*, the NER futile 5' processing of ICLs acts as a signal to recruit the unhooking activity.

Fill-in past the N^{4}C-ethyl-N^{4}C cross-link remnant was error-free as evidenced by the insertion of a guanine opposite the residual cytosine of the N^{4}C-ethyl-N^{4}C cross-linked remnant (Figure 5 and Figure 6). This result is consistent with that of Lloyd and coworkers who demonstrated that a cytosine was correctly placed opposite a N^{2}G-trimethylene-N^{2}G cross-link remnant by both human pol κ and *E. coli* pol IV (45,46).

Although the identity of the polymerase(s) involved in bypass of the N^{4}C-ethyl-N^{4}C remnant in mammalian cell extracts is not known, fill-in is aphidicolin sensitive (Figure S7). This observation suggests that one of the replicative polymerases (α, δ or ε) is involved in the repair synthesis step. It is not known whether the replicative polymerase stalls at the site of the cross-link remnant and requires a translesion polymerase to bypass the lesion, or if the replicative polymerase is able to carry out this step itself. However, *E. coli* Pol I and T7 DNA polymerase, both high fidelity polymerases (66), are able to bypass the N^{4}C-ethyl-N^{4}C remnant, a result that suggests mammalian replicative polymerases may also be able to bypass this lesion.

Bypass of the N3T-ethyl-N3T or N1I-ethyl-N3T remnant was not observed when duplexes containing these cross-links were incubated with mammalian cell extracts as determined by the α-^{32}P fill-in assay shown in Figure 4B. Instead a truncated product was observed, indicating that the polymerase stalled directly before the site of the cross-link remnant, a result consistent with the observed stall site of *E. coli* Pol I and T7 DNA polymerase in the primer extension assays (Figure 2). The high level of background inherent in the α-^{32}P fill-in assay may preclude observation of low levels of bypass of the T-T and I-T cross-link remnants. However, the phosphorothioate sequencing assay is very sensitive and has a relatively low background because the labeled 150mer is gel purified prior to iodine cleavage of the phosphorothioate bonds. Using this assay, we were unable to observe any repair patch when the T-T or I-T cross-linked duplexes were incubated in the XPF-deficient extracts (data not shown). This result indicates that, at least in the mammalian cell extracts used here, there is very little if any bypass of these ICL lesions.

We also prepared extracts using a modified Dignam procedure (67), a method that produces extracts that support translesion synthesis by polymerase η (68). These extracts were able to unhook both the N3T-ethyl-N3T and N3T-ethyl-N1I cross-links, but were not able to carry out repair synthesis (data not shown).

The α-^{32}P fill-in assay also failed to show repair synthesis past an AMT psoralen cross-linked duplex by the mammalian cell extracts. Although the psoralen remnant, which consists of

cyclobutane bridges between the pyrone and furan rings of psoralen and the 5–6 positions of two thymine rings, does not block the hydrogen bond face of the base, this adduct is quite bulky compared to the alkyl cross-links. It is this property that likely explains the lack of bypass of this lesion in the extracts. Application of the phosphorothioate sequencing assay failed to produce a repair patch when the AMT cross-linked duplex was incubated in an XPF-deficient extract (data not shown). These results are consistent with previous results that demonstrated repair synthesis took place up to, but not past the site of a psoralen cross-link in wild-type rodent cell (AA8) extracts (31). Furthermore, consistent with our data, it has recently been shown that *E. coli* Pol I and T4 DNA polymerase were almost completely blocked by a model psoralen remnant, although *E. coli* Pol I was able to bypass to a small extent (<1%) (15).

Our previously published results (30) demonstrated that independent of cross-link structure, cross-link induced distortions affect the ability of an ICL to be initially recognized and unhooked in mammalian cell extracts. The results presented here show that there are significant differences in the ability of cells to deal with ICLs and that these differences do depend on the chemical structure of the cross-link. This is consistent with earlier studies in *E. coli* suggesting psoralen ICLs are not repaired as efficiently as nitrogen mustard ICLs by a TLS dependent mechanism (11). An understanding of how the physical and chemical differences of interstrand cross-links affect the ability of the cell to repair this type of lesion may provide insights into how to design more effective cross-linking agents or lead to the development of strategies to prevent unwanted cross-link repair in tumor cells. Furthermore, information of this type may provide a better understanding of the cytotoxic and mutagenic potential of specific interstrand cross-links that are formed by endogenous and environmental agents.

Supplementary Material

Refer to Web version on PubMed Central for supplementary material.

Abbreviations

ICL, interstrand cross-link
NER, nucleotide excision repair
TLS, translesion synthesis
HR, homologous recombination
MMR, mismatch repair
FA, Fanconi anemia
DSB, double strand break
AMT, 4'-aminomethyl-4, 5',8-trimethyl-psoralen
TBE, Tris/Borate/EDTA
PNK, polynucleotide kinase
TE, Tris/EDTA
SAP, shrimp alkaline phosphatase
Kf, Klenow fragment
nt, nucleotide
bp, base pair

ACKNOWLEDGEMENTS

This research was supported by grants from the National Cancer Institute (CA082785, P.S.M.), the Natural Sciences and Engineering Research Council (NSERC, C.J.W.) of Canada. M.B.S was supported by a predoctoral fellowship from the American Heart Association (103527) and E.M.H. was supported by a training grant from the National Cancer Institute (T32 CA09110). We thank Ms. Maggie Wear for assistance in the preparation of oligonucleotides, and members of the Miller lab for many thoughtful discussions.

REFERENCES

1. Noll DM, Mason TM, Miller PS. Formation and repair of interstrand cross-links in DNA. Chem Rev 2006;106:277–301. [PubMed: 16464006]
2. Grillari J, Katinger H, Voglauer R. Contributions of DNA interstrand cross-links to aging of cells and organisms. Nucleic Acids Res 2007;35:7566–7576. [PubMed: 18083760]
3. Scharer OD. DNA interstrand crosslinks: natural and drug-induced DNA adducts that induce unique cellular responses. Chembiochem 2005;6:27–32. [PubMed: 15637664]
4. McHugh PJ, Spanswick VJ, Hartley JA. Repair of DNA interstrand crosslinks: molecular mechanisms and clinical relevance. Lancet Oncol 2001;2:483–490. [PubMed: 11905724]
5. Lehoczky P, McHugh PJ, Chovanec M. DNA interstrand cross-link repair in Saccharomyces cerevisiae. FEMS Microbiol Rev 2007;31:109–133. [PubMed: 17096663]
6. Cole RS, Sinden RR. Repair of cross-linked DNA in Escherichia coli. Basic Life Sci 1975;5B:487–495. [PubMed: 1103865]
7. Cole RS. Repair of DNA containing interstrand crosslinks in Escherichia coli: sequential excision and recombination. Proc Natl Acad Sci U S A 1973;70:1064–1068. [PubMed: 4577788]
8. Saffran WA, Ahmed S, Bellevue S, Pereira G, Patrick T, Sanchez W, Thomas S, Alberti M, Hearst JE. DNA repair defects channel interstrand DNA cross-links into alternate recombinational and error-prone repair pathways. J Biol Chem 2004;279:36462–36469. [PubMed: 15213235]
9. Zheng H, Wang X, Warren AJ, Legerski RJ, Nairn RS, Hamilton JW, Li L. Nucleotide excision repair- and polymerase eta-mediated error-prone removal of mitomycin C interstrand cross-links. Mol Cell Biol 2003;23:754–761. [PubMed: 12509472]
10. Wang X, Peterson CA, Zheng H, Nairn RS, Legerski RJ, Li L. Involvement of nucleotide excision repair in a recombination-independent and error-prone pathway of DNA interstrand cross-link repair. Mol Cell Biol 2001;21:713–720. [PubMed: 11154259]
11. Berardini M, Mackay W, Loechler EL. Evidence for a recombination-independent pathway for the repair of DNA interstrand cross-links based on a site-specific study with nitrogen mustard. Biochemistry 1997;36:3506–3513. [PubMed: 9132000]
12. Sarkar S, Davies AA, Ulrich HD, McHugh PJ. DNA interstrand crosslink repair during G1 involves nucleotide excision repair and DNA polymerase zeta. Embo J 2006;25:1285–1294. [PubMed: 16482220]
13. Richards S, Liu ST, Majumdar A, Liu JL, Nairn RS, Bernier M, Maher V, Seidman MM. Triplex targeted genomic crosslinks enter separable deletion and base substitution pathways. Nucleic Acids Res 2005;33:5382–5393. [PubMed: 16186129]
14. Cheng S, Sancar A, Hearst JE. RecA-dependent incision of psoralen-crosslinked DNA by (A)BC excinuclease. Nucleic Acids Res 1991;19:657–663. [PubMed: 2011535]
15. Zietlow L, Bessho T. DNA polymerase I-mediated translesion synthesis in RecA-independent DNA interstrand cross-link repair in E. coli. Biochemistry 2008;47:5460–5464. [PubMed: 18416557]
16. Bessho T, Mu D, Sancar A. Initiation of DNA interstrand cross-link repair in humans: the nucleotide excision repair system makes dual incisions 5' to the cross-linked base and removes a 22- to 28-nucleotide-long damage-free strand. Mol Cell Biol 1997;17:6822–6830. [PubMed: 9372913]
17. Thoma BS, Wakasugi M, Christensen J, Reddy MC, Vasquez KM. Human XPC-hHR23B interacts with XPA-RPA in the recognition of triplex-directed psoralen DNA interstrand crosslinks. Nucleic Acids Res 2005;33:2993–3001. [PubMed: 15914671]
18. Liu Y, Nairn RS, Vasquez KM. Processing of triplex-directed psoralen DNA interstrand crosslinks by recombination mechanisms. Nucleic Acids Res 2008;36:4680–4688. [PubMed: 18628293]
19. De Silva IU, McHugh PJ, Clingen PH, Hartley JA. Defining the roles of nucleotide excision repair and recombination in the repair of DNA interstrand cross-links in mammalian cells. Mol Cell Biol 2000;20:7980–7990. [PubMed: 11027268]
20. Mogi S, Butcher CE, Oh DH. DNA polymerase eta reduces the gamma-H2AX response to psoralen interstrand crosslinks in human cells. Exp Cell Res 2008;314:887–895. [PubMed: 18068156]
21. Misra RR, Vos JM. Defective replication of psoralen adducts detected at the gene-specific level in xeroderma pigmentosum variant cells. Mol Cell Biol 1993;13:1002–1012. [PubMed: 8423773]

22. Shen X, Jun S, O'Neal LE, Sonoda E, Bemark M, Sale JE, Li L. REV3 and REV1 play major roles in recombination-independent repair of DNA interstrand cross-links mediated by monoubiquitinated proliferating cell nuclear antigen (PCNA). J Biol Chem 2006;281:13869–13872. [PubMed: 16571727]
23. Wu Q, Christensen LA, Legerski RJ, Vasquez KM. Mismatch repair participates in error-free processing of DNA interstrand crosslinks in human cells. EMBO Rep 2005;6:551–557. [PubMed: 15891767]
24. Zhang N, Lu X, Zhang X, Peterson CA, Legerski RJ. hMutSbeta is required for the recognition and uncoupling of psoralen interstrand cross-links in vitro. Mol Cell Biol 2002;22:2388–2397. [PubMed: 11884621]
25. Zhao J, Jain A, Iyer RR, Modrich PL, Vasquez KM. Mismatch repair and nucleotide excision repair proteins cooperate in the recognition of DNA interstrand crosslinks. Nucleic Acids Res 2009;37in press
26. Andreassen PR, Ren K. Fanconi anemia proteins, DNA interstrand crosslink repair pathways, and cancer therapy. Curr Cancer Drug Targets 2009;9:101–117. [PubMed: 19200054]
27. Hanada K, Budzowska M, Modesti M, Maas A, Wyman C, Essers J, Kanaar R. The structure-specific endonuclease Mus81-Eme1 promotes conversion of interstrand DNA crosslinks into double-strands breaks. Embo J 2006;25:4921–4932. [PubMed: 17036055]
28. Cheng WH, Muftic D, Muftuoglu M, Dawut L, Morris C, Helleday T, Shiloh Y, Bohr VA. WRN is required for ATM activation and the S-phase checkpoint in response to interstrand cross-link-induced DNA double-strand breaks. Mol Biol Cell 2008;19:3923–3933. [PubMed: 18596239]
29. Cheng WH, Kusumoto R, Opresko PL, Sui X, Huang S, Nicolette ML, Paull TT, Campisi J, Seidman M, Bohr VA. Collaboration of Werner syndrome protein and BRCA1 in cellular responses to DNA interstrand cross-links. Nucleic Acids Res 2006;34:2751–2760. [PubMed: 16714450]
30. Smeaton MB, Hlavin EM, McGregor Mason T, Noronha AM, Wilds CJ, Miller PS. Distortion-dependent unhooking of interstrand cross-links in mammalian cell extracts. Biochemistry 2008;47:9920–9930. [PubMed: 18702509]
31. Mu D, Bessho T, Nechev LV, Chen DJ, Harris TM, Hearst JE, Sancar A. DNA interstrand cross-links induce futile repair synthesis in mammalian cell extracts. Mol Cell Biol 2000;20:2446–2454. [PubMed: 10713168]
32. Wilds CJ, Xu F, Noronha AM. Synthesis and characterization of DNA containing an N1-2' -deoxyinosine-ethyl-N3-thymidine interstrand cross-link: a structural mimic of the cross-link formed by 1,3-bis-(2-chloroethyl)-1-nitrosourea. Chem Res Toxicol 2008;21:686–695. [PubMed: 18257558]
33. Wilds CJ, Noronha AM, Robidoux S, Miller PS. Mispair-aligned N3T-alkyl-N3T interstrand cross-linked DNA: synthesis and characterization of duplexes with interstrand cross-links of variable lengths. J Am Chem Soc 2004;126:9257–9265. [PubMed: 15281815]
34. Noronha AM, Noll DM, Wilds CJ, Miller PS. N(4)C-ethyl-N(4)C cross-linked DNA: synthesis and characterization of duplexes with interstrand cross-links of different orientations. Biochemistry 2002;41:760–761. [PubMed: 11790097]
35. Noll DM, Webba da Silva M, Noronha AM, Wilds CJ, Colvin OM, Gamcsik MP, Miller PS. Structure, flexibility, and repair of two different orientations of the same alkyl interstrand DNA cross-link. Biochemistry 2005;44:6764–6775. [PubMed: 15865422]
36. Mason TM, Smeaton MB, Cheung JC, Hanakahi LA, Miller PS. End modification of a linear DNA duplex enhances NER-mediated excision of an internal Pt(II)-lesion. Bioconjug Chem 2008;19:1064–1070. [PubMed: 18447369]
37. Smeaton MB, Miller PS, Ketner G, Hanakahi LA. Small-scale extracts for the study of nucleotide excision repair and non-homologous end joining. Nucleic Acids Res 2007;35:e152. [PubMed: 18073193]
38. Noll DM, Noronha AM, Miller PS. Synthesis and characterization of DNA duplexes containing an N(4)C-ethyl-N(4)C interstrand cross-link. J Am Chem Soc 2001;123:3405–3411. [PubMed: 11472110]
39. Manley JL, Fire A, Samuels M, Sharp PA. In vitro transcription: whole-cell extract. Methods Enzymol 1983;101:568–582. [PubMed: 6193397]

40. Reardon JT, Sancar A. Purification and characterization of Escherichia coli and human nucleotide excision repair enzyme systems. Methods Enzymol 2006;408:189–213. [PubMed: 16793370]
41. Gish G, Eckstein F. DNA and RNA sequence determination based on phosphorothioate chemistry. Science 1988;240:1520–1522. [PubMed: 2453926]
42. Reardon JT, Thompson LH, Sancar A. Rodent UV-sensitive mutant cell lines in complementation groups 6–10 have normal general excision repair activity. Nucleic Acids Res 1997;25:1015–1021. [PubMed: 9023113]
43. Sibghat U, Sancar A, Hearst JE. The repair patch of E. coli (A) BC excinuclease. Nucleic Acids Res 1990;18:5051–5053. [PubMed: 2205836]
44. Noronha AM, Noll DM, Miller PS. Syntheses of DNA duplexes containing a C-C interstrand cross-link. Nucleosides Nucleotides Nucleic Acids 2001;20:1303–1307. [PubMed: 11563009]
45. Minko IG, Harbut MB, Kozekov ID, Kozekova A, Jakobs PM, Olson SB, Moses RE, Harris TM, Rizzo CJ, Lloyd RS. Role for DNA polymerase kappa in the processing of N2-N2-guanine interstrand cross-links. J Biol Chem 2008;283:17075–17082. [PubMed: 18434313]
46. Kumari A, Minko IG, Harbut MB, Finkel SE, Goodman MF, Lloyd RS. Replication bypass of interstrand cross-link intermediates by Escherichia coli DNA polymerase IV. J Biol Chem 2008;283:27433–27437. [PubMed: 18697749]
47. Niedernhofer LJ, Daniels JS, Rouzer CA, Greene RE, Marnett LJ. Malondialdehyde, a product of lipid peroxidation, is mutagenic in human cells. J Biol Chem 2003;278:31426–31433. [PubMed: 12775726]
48. Summerfield FW, Tappel AL. Detection and measurement by high-performance liquid chromatography of malondialdehyde crosslinks in DNA. Anal Biochem 1984;143:265–271. [PubMed: 6532242]
49. Stone MP, Cho YJ, Huang H, Kim HY, Kozekov ID, Kozekova A, Wang H, Minko IG, Lloyd RS, Harris TM, Rizzo CJ. Interstrand DNA cross-links induced by alpha,beta-unsaturated aldehydes derived from lipid peroxidation and environmental sources. Acc Chem Res 2008;41:793–804. [PubMed: 18500830]
50. Kozekov ID, Nechev LV, Moseley MS, Harris CM, Rizzo CJ, Stone MP, Harris TM. DNA interchain cross-links formed by acrolein and crotonaldehyde. J Am Chem Soc 2003;125:50–61. [PubMed: 12515506]
51. Caulfield JL, Wishnok JS, Tannenbaum SR. Nitric oxide-induced interstrand cross-links in DNA. Chem Res Toxicol 2003;16:571–574. [PubMed: 12755585]
52. Sczepanski JT, Jacobs AC, Greenberg MM. Self-promoted DNA interstrand cross-link formation by an abasic site. J Am Chem Soc 2008;130:9646–9647. [PubMed: 18593126]
53. McHugh PJ, Sarkar S. DNA interstrand cross-link repair in the cell cycle: a critical role for polymerase zeta in G1 phase. Cell Cycle 2006;5:1044–1047. [PubMed: 16687932]
54. Liu X, Lao Y, Yang IY, Hecht SS, Moriya M. Replication-coupled repair of crotonaldehyde/acetaldehyde-induced guanine-guanine interstrand cross-links and their mutagenicity. Biochemistry 2006;45:12898–12905. [PubMed: 17042508]
55. Cipak L, Watanabe N, Bessho T. The role of BRCA2 in replication-coupled DNA interstrand cross-link repair in vitro. Nat Struct Mol Biol 2006;13:729–733. [PubMed: 16845393]
56. Fisher LA, Bessho M, Bessho T. Processing of a psoralen DNA interstrand cross-link by XPF-ERCC1 complex in vitro. J Biol Chem 2008;283:1275–1281. [PubMed: 18006494]
57. Kuraoka I, Kobertz WR, Ariza RR, Biggerstaff M, Essigmann JM, Wood RD. Repair of an interstrand DNA cross-link initiated by ERCC1-XPF repair/recombination nuclease. J Biol Chem 2000;275:26632–26636. [PubMed: 10882712]
58. Niedernhofer LJ, Odijk H, Budzowska M, van Drunen E, Maas A, Theil AF, de Wit J, Jaspers NG, Beverloo HB, Hoeijmakers JH, Kanaar R. The structure-specific endonuclease Ercc1-Xpf is required to resolve DNA interstrand cross-link-induced double-strand breaks. Mol Cell Biol 2004;24:5776–5787. [PubMed: 15199134]
59. Ahmad A, Robinson AR, Duensing A, van Drunen E, Beverloo HB, Weisberg DB, Hasty P, Hoeijmakers JH, Niedernhofer LJ. ERCC1-XPF endonuclease facilitates DNA double-strand break repair. Mol Cell Biol 2008;28:5082–5092. [PubMed: 18541667]

60. Li L, Peterson CA, Lu X, Wei P, Legerski RJ. Interstrand cross-links induce DNA synthesis in damaged and undamaged plasmids in mammalian cell extracts. Mol Cell Biol 1999;19:5619–5630. [PubMed: 10409751]

61. Li L, Peterson CA, Zhang X, Legerski RJ. Requirement for PCNA and RPA in interstrand crosslink-induced DNA synthesis. Nucleic Acids Res 2000;28:1424–1427. [PubMed: 10684938]

62. Zhang N, Kaur R, Lu X, Shen X, Li L, Legerski RJ. The Pso4 mRNA splicing and DNA repair complex interacts with WRN for processing of DNA interstrand cross-links. J Biol Chem 2005;280:40559–40567. [PubMed: 16223718]

63. Zhang N, Liu X, Li L, Legerski R. Double-strand breaks induce homologous recombinational repair of interstrand cross-links via cooperation of MSH2, ERCC1-XPF, REV3, and the Fanconi anemia pathway. DNA Repair (Amst) 2007;6:1670–1678. [PubMed: 17669695]

64. Swenson MC, Paranawithana SR, Miller PS, Kielkopf CL. Structure of a DNA repair substrate containing an alkyl interstrand cross-link at 1.65 A resolution. Biochemistry 2007;46:4545–4553. [PubMed: 17375936]

65. Raschle M, Knipsheer P, Enoiu M, Angelov T, Sun J, Griffith JD, Ellenberger TE, Scharer OD, Walter JC. Mechanism of replication-coupled DNA interstrand crosslink repair. Cell 2008;134:969–980. [PubMed: 18805090]

66. McCulloch SD, Kunkel TA. The fidelity of DNA synthesis by eukaryotic replicative and translesion synthesis polymerases. Cell Res 2008;18:148–161. [PubMed: 18166979]

67. Dignam JD, Lebovitz RM, Roeder RG. Accurate transcription initiation by RNA polymerase II in a soluble extract from isolated mammalian nuclei. Nucleic Acids Res 1983;11:1475–1489. [PubMed: 6828386]

68. Cordonnier AM, Lehmann AR, Fuchs RP. Impaired translesion synthesis in xeroderma pigmentosum variant extracts. Mol Cell Biol 1999;19:2206–2211. [PubMed: 10022907]

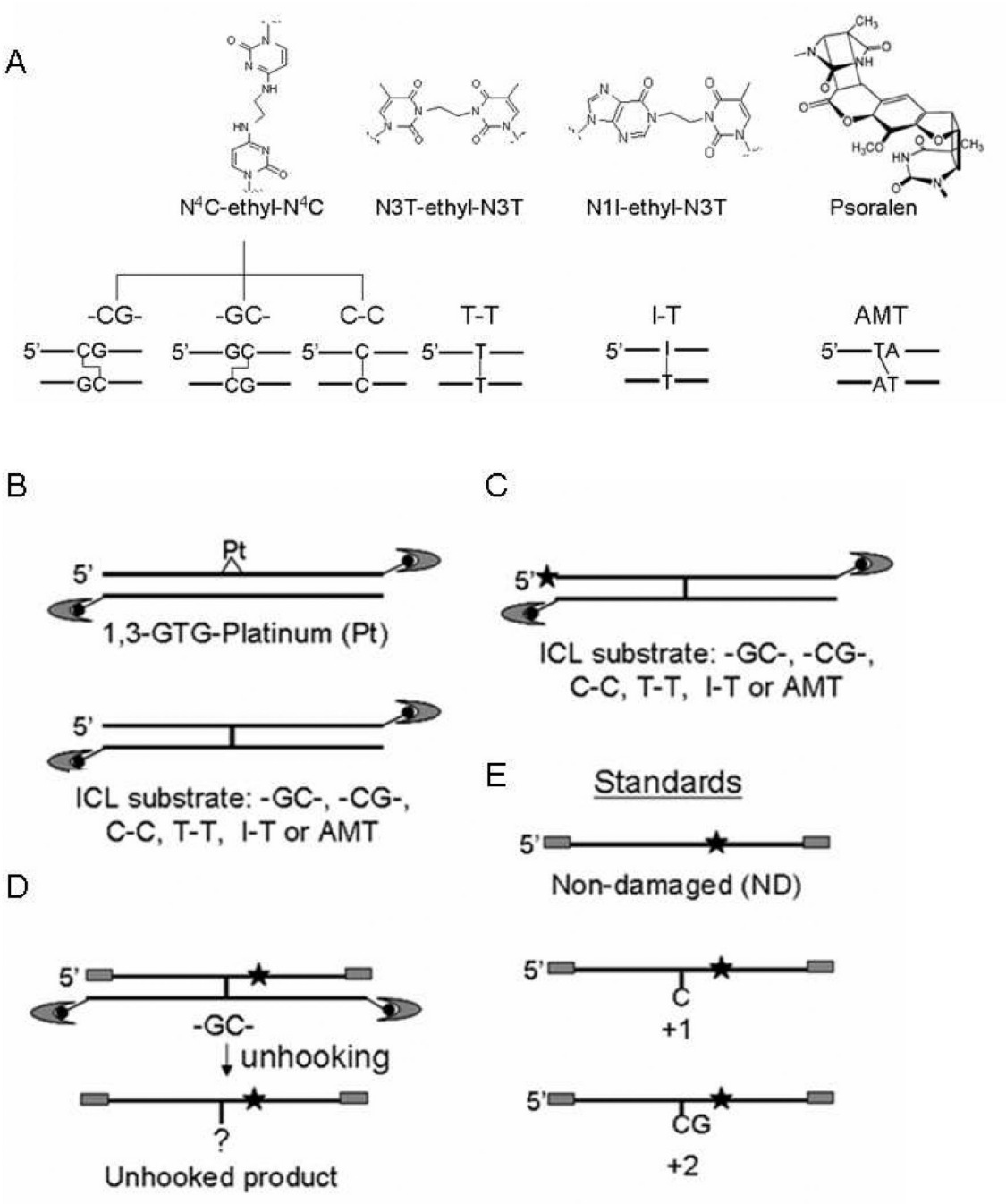

Figure 1.

Schematic of substrates used in this study. (A) Interstrand cross-linked substrates used in this study. The N^4C-ethyl-N^4C cross-link retains the ability to hydrogen bond correctly with a guanine, whereas the N3T-ethyl-N3T and N1I-ethyl-N3T cross-links block the hydrogen bonding face of the adducted bases. Schematics of the duplexes are shown beneath the abbreviations used for each cross-link. (B) Substrates used in the α-^{32}P repair synthesis assays are unlabeled and contain a 3' biotin (black dot) that is conjugated to streptavidin (gray half moon) before incubation with cellular extracts. (C) Substrates used in the phosphorothioate sequencing assays. These substrates are labeled with ^{32}P (star) at 6000 Ci/mmol at the 5' end of duplex **A**. (D) -GC- substrate used to isolate unhooked product. These substrates contain

the ^{32}P label (star) at the junction of **X** and **D** duplexes in the top strand. The top strand contains 5 or 6 contiguous methylphosphonate linkages at the 5’ or the 3’ end, respectively (as denoted with gray bar). The biotin/streptavidin conjugates are located on either end of the duplex on the bottom strand. The schematic of the labeled unhooked product is shown with a question mark to indicate that the number of nucleotides attached to the cross-link remnant was unknown. (E) Standards used to compare to the unhooked product, showing only the labeled top strand that is observed for clarity. These standards are the same length and sequence composition of the -GC- unhooked product and also contain the same terminal methylphosphonate modifications (gray bars).

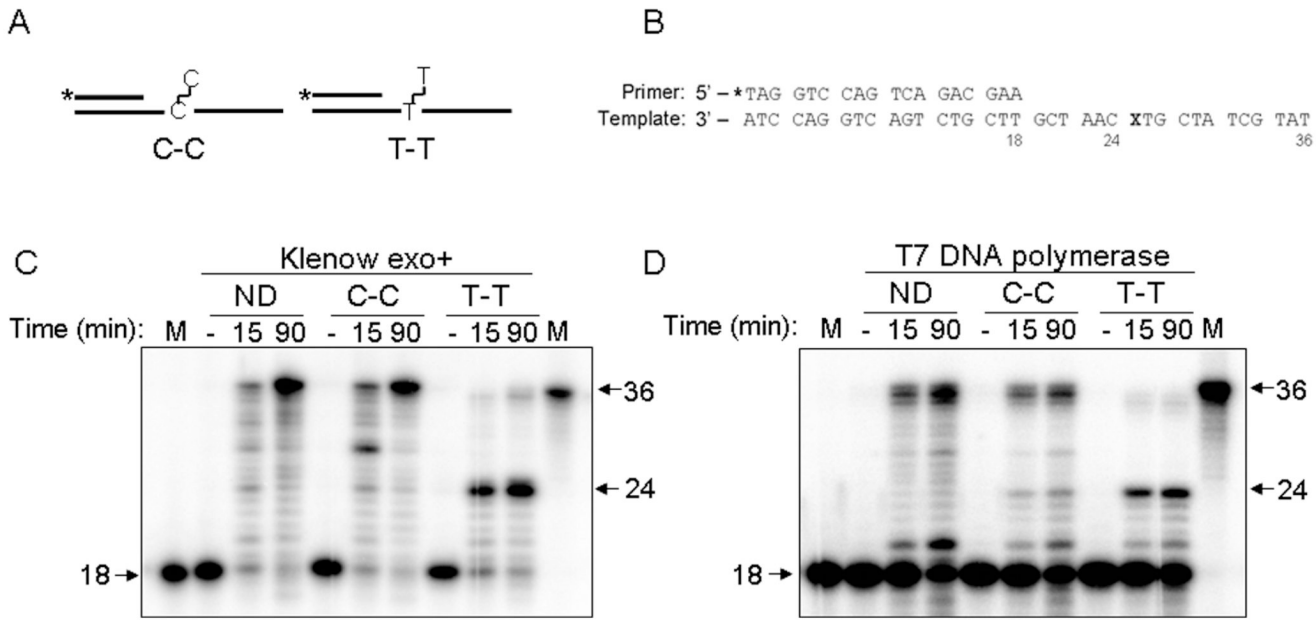

Figure 2.

Primer extension assay with *E. coli* Pol I and T7 DNA polymerase. (A) Schematic of the substrates used in the assay. Each template strand contains a site-specific single base cross-link remnant. Star = ^{32}P label (B) Sequences of the primer and template used in the assay. The X denotes the placement of a non-damaged cytosine as a control, a N^4C-ethyl-N^4C cross-link or a N3T-ethyl-N3T cross-link. The numbers beneath the sequence denote the primer length (18mer), the full length polymerization product (36mer) or the length of the product generated when DNA polymerase stalls at the cross-link remnant site (24mer). (C) Primer extension with *E. coli* Pol I Klenow fragment exo+. M indicates molecular weight markers. (D) Primer extension using T7 DNA polymerase.

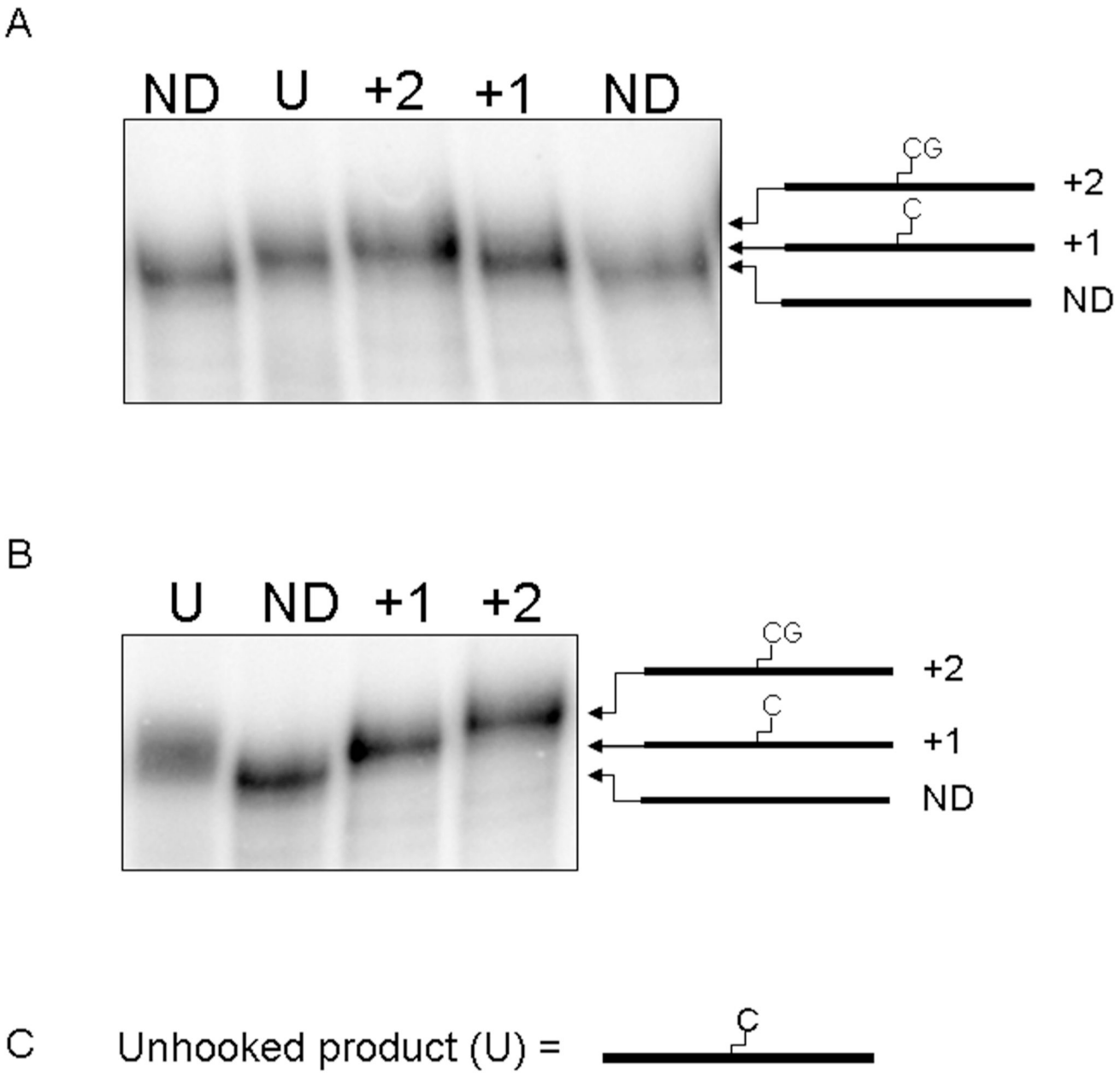

Figure 3.

Characterization of the cross-link remnant generated by unhooking in mammalian cell extracts. Unhooking was carried out using a -GC- cross-linked duplex, shown schematically in Figure 1D, in either (A) HeLa extract or (B) CHO AA8 extract. The unhooked product (U) was purified as described in Experimental Procedures. The mobility of the unhooked product was compared to standards of the same length and sequence composition containing no damage (ND), a single cross-linked cytosine (**+1**) or a cross-linked CG (**+2**) shown schematically in Figure 1E. The unhooked product from both HeLa and rodent cell extracts has only a single base attached, as shown schematically in (C).

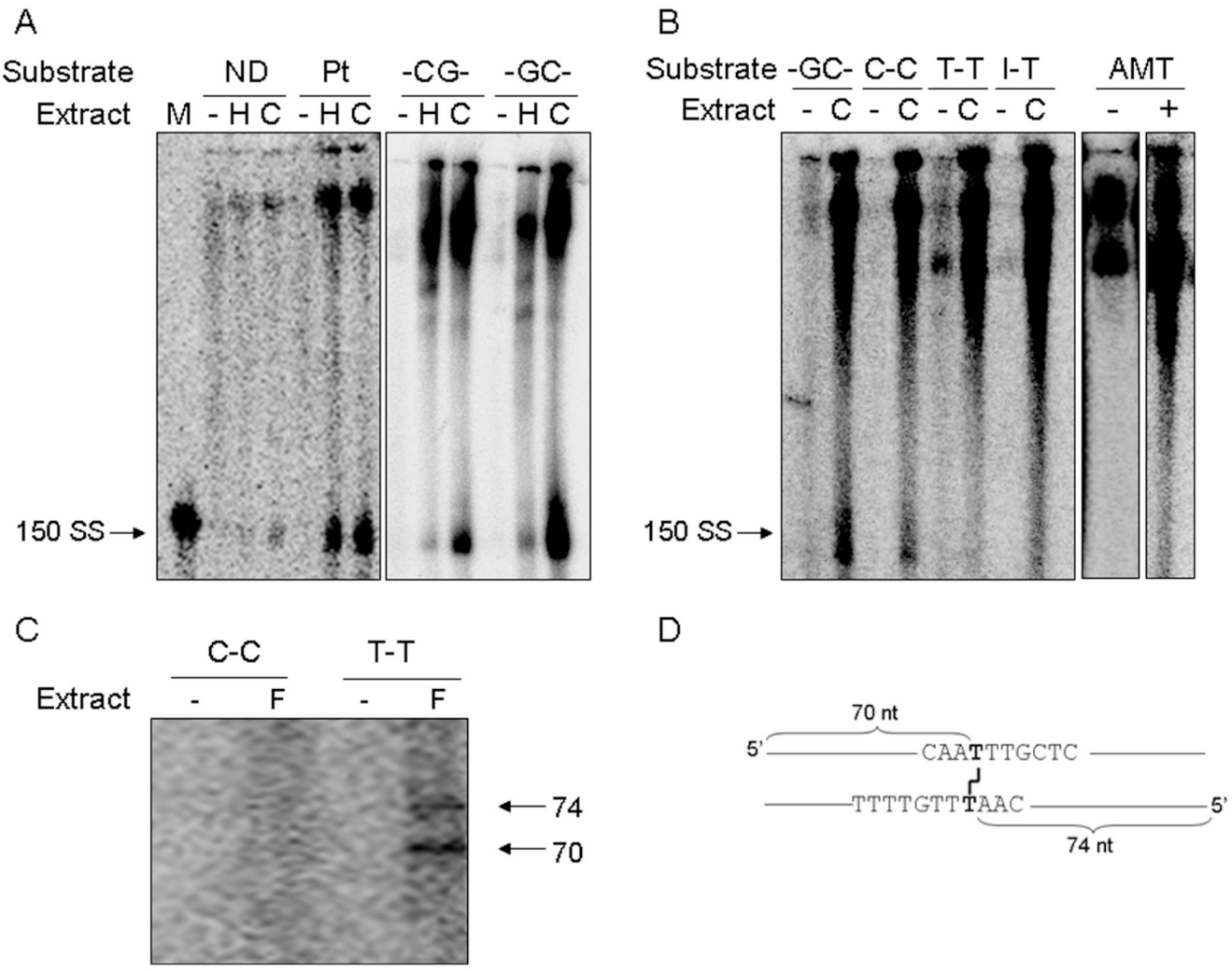

Figure 4.

Repair synthesis assays on cross-linked duplexes in mammalian cell extracts. The duplexes used in the repair synthesis assays are shown in Figure 1B. (A) ^{32}P incorporation into 150mer product was monitored on a 6% denaturing gel using unlabeled duplexes that contained either no damage (ND), a 1,3-(GTG) platinum lesion (Pt), the -CG- or the -GC- cross-links when incubated with HeLa (H) or CHO AA8 (C) extracts. (B) Repair synthesis assays in CHO AA8 extracts using duplexes that contain a N^4C-ethyl-N^4C (-GC- and C-C), a N3T-ethyl-N3T (T-T), a N1I-ethyl-N3T (I-T) or psoralen (AMT) ICL. (C) Repair synthesis assays in no extract (-) or in an XPF-deficient extract (F) using the C-C and T-T cross-linked duplexes. The products of these reactions were analyzed on an 8% sequencing gel. (D) Size of truncated polymerization products from (C) indicates the polymerase stalls at the T-T cross-link remnant as a result of polymerization on either the top or bottom strand.

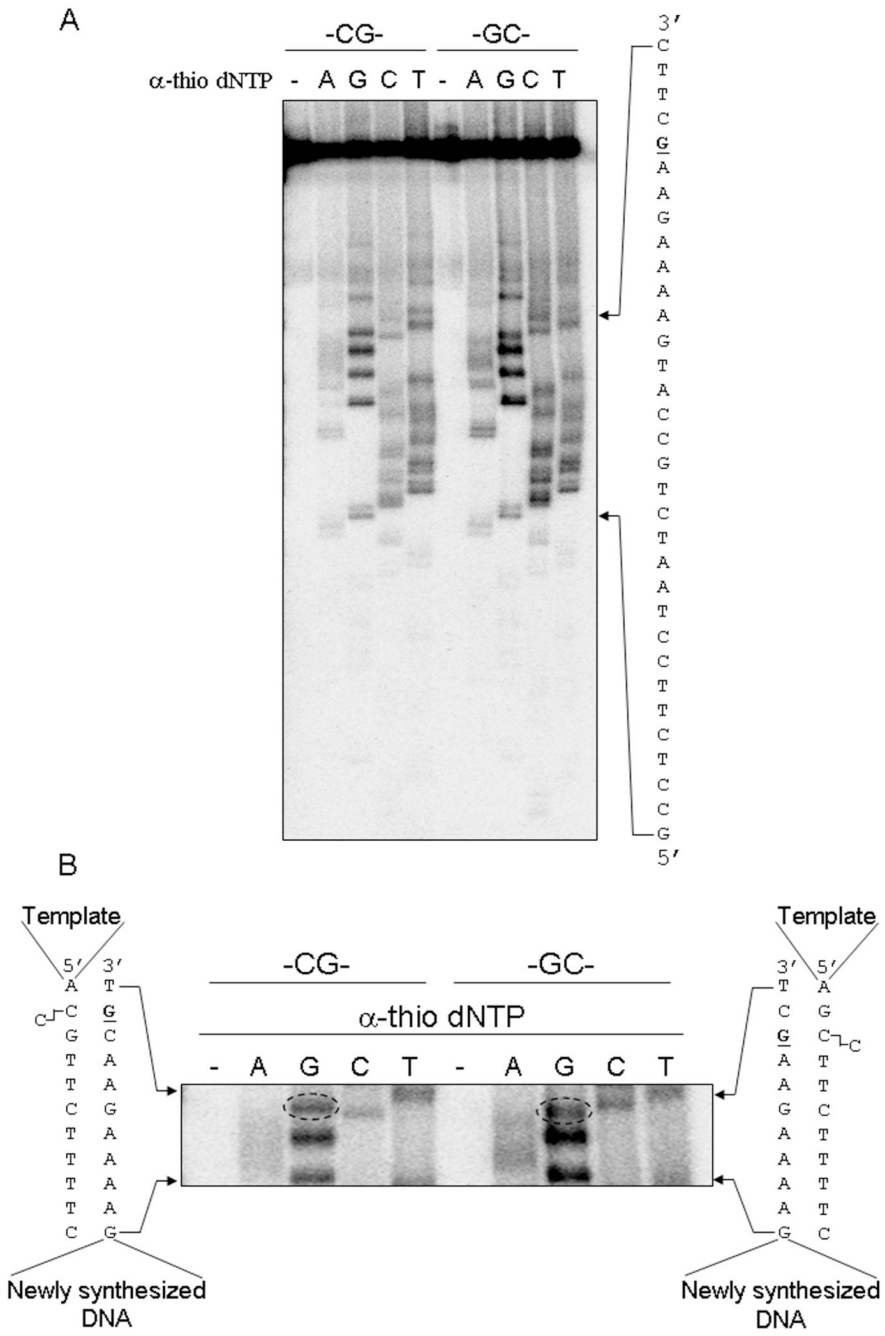

Figure 5.

Phosphorothioate sequencing assay in wild-type cell extract using duplexes that contain a -CG- or -GC- oriented N^4C-ethyl-N^4C ICL. The structures of the cross-linked duplexes are shown schematically in Figure 1C. (A) Repair patch generated by the -CG- and -GC- cross-linked duplexes. The sequence of the repair patch from the -GC- duplex is shown to the right of the gel, where the underlined guanine is the base incorporated opposite the N^4C-ethyl-N^4C cross-link remnant. (B) Enlarged view of the repair patch surrounding the site of the cross-link. The dashed circle encloses the guanine that was inserted opposite the N^4C-ethyl-N^4C cross-link. The sequences to the side of the gel show the unhooked product template and the newly synthesized DNA sequence surrounding the site of the cross-link.

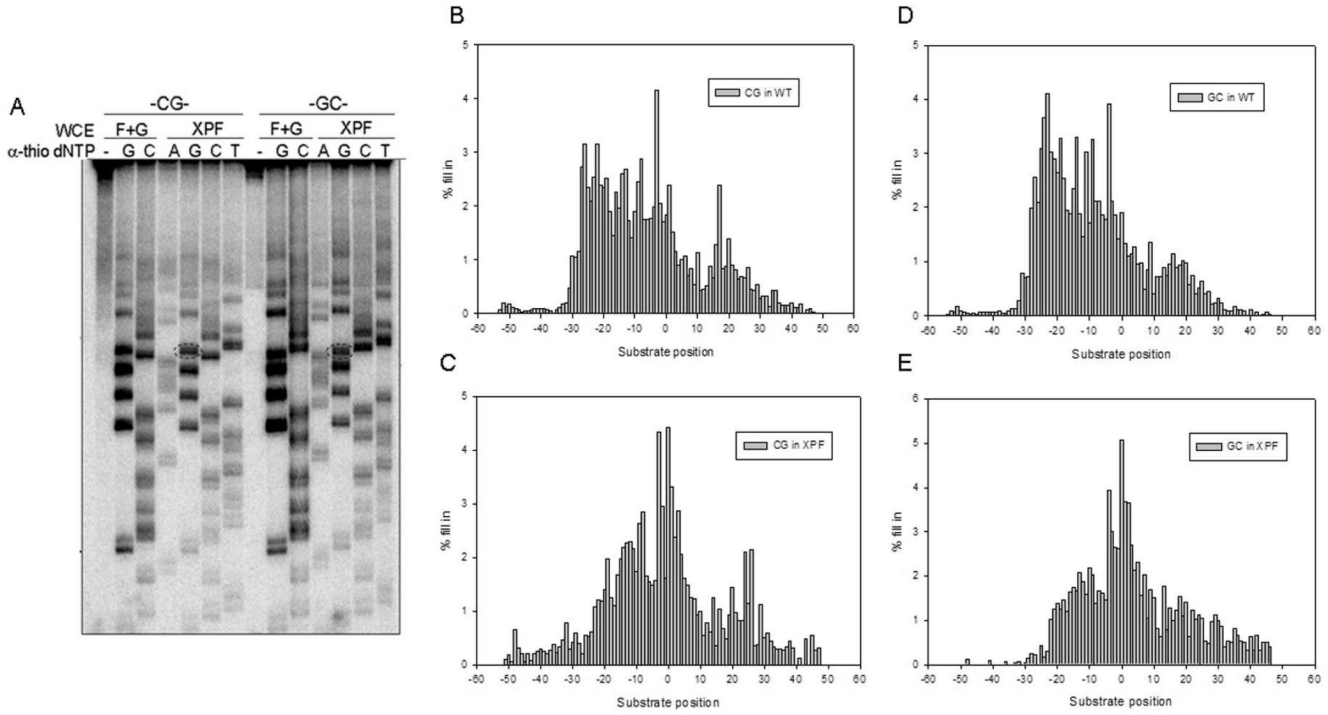

Figure 6.

Phosphorothioate sequencing assay in NER-deficient cell extract using duplexes that contain a -CG- or -GC- oriented N^4C-ethyl-N^4C ICL. (A) The -CG- or -GC- cross-linked duplexes shown schematically in Figure 1C were incubated with complemented XPF-deficient and XPG-deficient extracts (F+G) that are functionally wild-type for NER activity or with an NER-deficient XPF extract. The dashed circle encloses the guanine inserted opposite the N^4C-ethyl-N^4C cross-link. (B–E) Quantification of repair patch. (B and D) NER-dependent repair patch in wild-type rodent extract on -CG- or -GC- cross-linked duplexes, respectively. (C and E) NER-independent repair patch when -CG- or -GC- cross-linked duplexes are incubated with XPF extracts, respectively. Loss of repair synthesis beginning at the −28 position is apparent in the XPF mutant extracts although a smaller patch surrounding the cross-link site still exists.

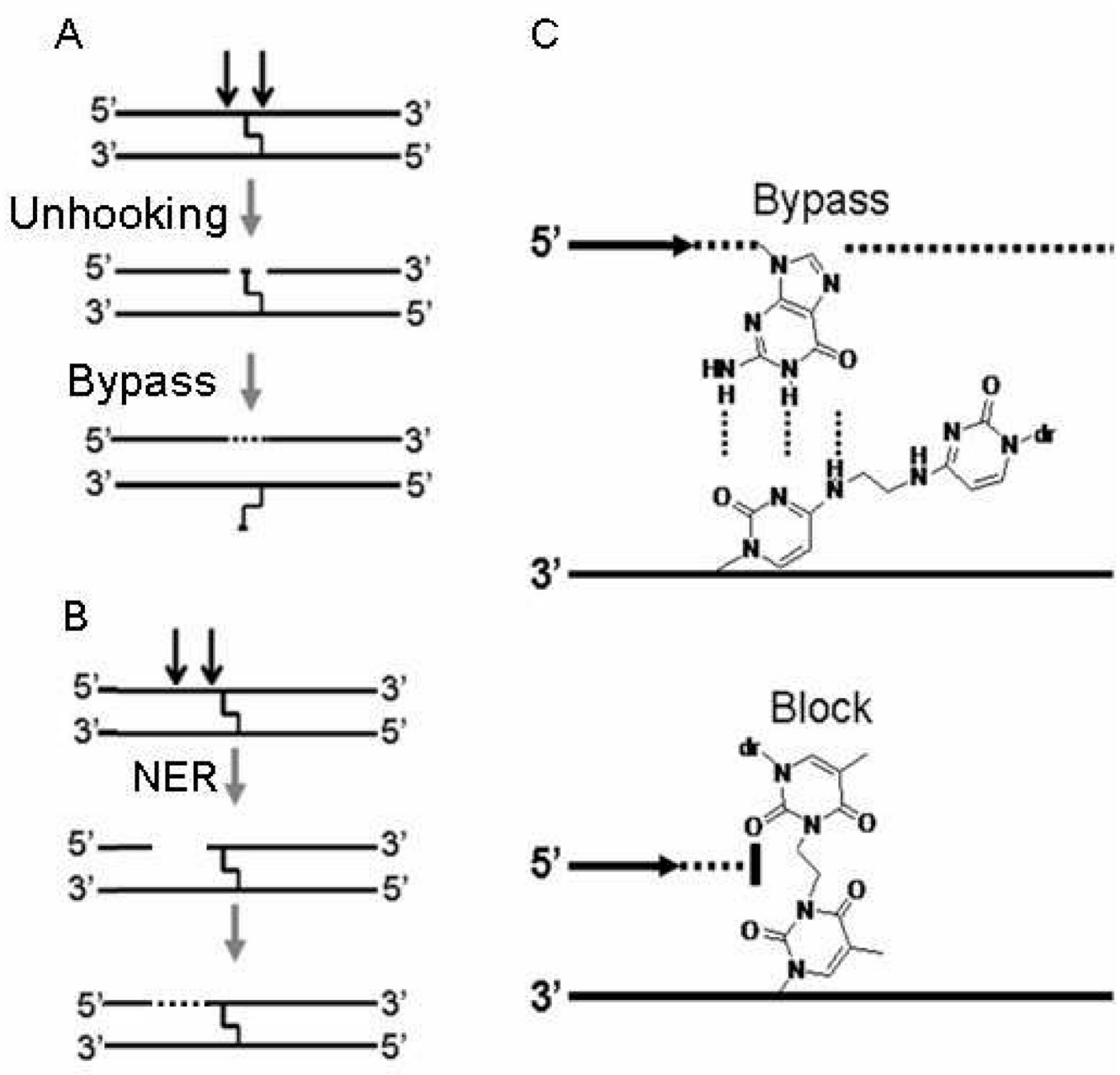

Figure 7.

(A) Schematic of unhooking and lesion bypass events that occur to repair ICLs in the absence of a homologous donor sequence. (B) Schematic of NER dual 5' incisions and resulting repair synthesis, leaving the cross-link intact. Note that the repair synthesis process may result in ligation to regenerate the cross-linked species or undergo a futile repair synthesis process as described in ref (31). (C) Schematic of the interstrand cross-links remnants and how their structure affects DNA polymerase bypass. The N^4C-ethyl-N^4C cross-link retains hydrogen bonding potential and allows error-free polymerase bypass while the N3T-ethyl-N3T cross-link blocks the hydrogen bond face and impedes polymerase bypass.